

System identification of a super high-rise building via a stochastic subspace approach

Lucia Faravelli^{1a}, Filippo Ubertini^{*2} and Clemente Fuggini^{3b}

¹Department of Structural Mechanics, University of Pavia, Pavia, Italy

²Department of Civil and Environmental Engineering, University of Perugia, Perugia, Italy

³Research & Innovation Division, D'Appolonia S.P.A., Genova, Italy

(Received May 7, 2010, Accepted November 4, 2010)

Abstract. System identification is a fundamental step towards the application of structural health monitoring and damage detection techniques. On this respect, the development of evolved identification strategies is a priority for obtaining reliable and repeatable baseline modal parameters of an undamaged structure to be adopted as references for future structural health assessments. The paper presents the identification of the modal parameters of the Guangzhou New Television Tower, China, using a data-driven stochastic subspace identification (SSI-data) approach complemented with an appropriate automatic mode selection strategy which proved to be successful in previous literature studies. This well-known approach is based on a clustering technique which is adopted to discriminate structural modes from spurious noise ones. The method is applied to the acceleration measurements made available within the task I of the ANCRiSST benchmark problem, which cover 24 hours of continuous monitoring of the structural response under ambient excitation. These records are then subdivided into a convenient number of data sets and the variability of modal parameter estimates with ambient temperature and mean wind velocity are pointed out. Both 10 minutes and 1 hour long records are considered for this purpose. A comparison with finite element model predictions is finally carried out, using the structural matrices provided within the benchmark, in order to check that all the structural modes contained in the considered frequency interval are effectively identified via SSI-data.

Keywords: system identification; field measurements; stochastic subspace decomposition; environmental effects; finite element analysis.

1. Introduction

System identification is an open research field with considerable potentialities within the subjects of structural health assessment (Frizzarin *et al.* 2008, Gentile and Gallino 2008, Hong *et al.* 2009) and structural control (Casciati and Ubertini 2008, Ubertini 2008a, Faravelli *et al.* 2009a, Faravelli *et al.* 2009b). In the former case, most of the efforts are currently being devoted to using data recorded by permanent vibration monitoring systems for detecting and quantifying damage and for estimating the residual service life of the structure. These strategies are particularly useful in the case of strategic structures such as long-span bridges (Wong 2004, Ko and Ni 2005, Conte *et al.*

*Corresponding Author, Assistant Professor, E-mail: filippo.ubertini@strutture.unipg.it

^aFull Professor

^bResearch Scholar

2008) and tall buildings. The use of innovative sensors, such as Global Positioning Systems (GPS), is also worth mentioning (Ni *et al.* 2009, Fuggini 2009). On this respect, recent literature works (Chatzi and Smyth 2009) shown that displacement records might be effectively employed together with acceleration measurements for identification purposes of strongly nonlinear systems (Faravelli and Ubertini 2009) using appropriate algorithms.

According to many authors (Van Overschee and De Moor 1996, Peeters and De Roeck 2000, Alicioğlu and Lus 2008, Faravelli *et al.* 2010), data-driven stochastic subspace identification (SSI-data) is the most advanced class of algorithms currently available for time domain operational modal analysis of structures. One recognized merit of these techniques is indeed the fact that they do not require well-separated and low damping modes, which on the contrary are necessary assumptions in the case of methods like the Peak Peaking Method. Consequently, SSI techniques are able to identify modes even with very close frequencies and with virtually any value of the damping ratios (Peeters and Ventura 2003, Ren *et al.* 2005). Applications of SSI methods to damage detection were already presented in the literature (Weng *et al.* 2009). The use of such methods requires some data preconditioning tricks, the tuning of some fundamental parameters (Pridham and Wilson 2005) and the implementation of appropriate rules for separating structural modes from spurious noise ones (Alicioğlu and Lus 2008). Unfortunately, these steps are far from being straightforward and it is not unusual that different analysts come out with different modal parameter estimates using the same raw data. For this reason, benchmark problems for system identification represent quite profitable opportunities to test the effectiveness of different identification techniques.

Two main concerns in structural identification are: the analysis of the variability of the results and the influence of environmental effects on the predicted modal properties. These two aspects are directly related to the resolution of damage detection techniques. Indeed, the minimum level of damage that can be identified is the one that determines the minimal variation of some damage index which is not hidden by random variations nor by environmental effects. A method for estimating the complete covariance matrix of the system parameters identified via SSI was recently presented by Reynders *et al.* (2008), who proposed to remove the bias of the identified system model and provided expressions of the covariances of modal parameters. Some open issues in determining confidence intervals of estimated modal parameters using SSI methods were also discussed by Carden and Mita (2009), who shown that for reasonable data lengths, the knowledge of the covariance might not be sufficient to compute reliable confidence intervals. Indeed, if the data lengths are not sufficiently large, which is usually the case of flexible structures (with natural frequencies below 1 Hz), the modal parameter estimates might exhibit non-normal distributions. On the other hand, the obtained confidence intervals are naturally affected by inherent statistical errors, such as nonlinearities and non-stationarity, which might be enhanced in the case of long data records. The influence of environmental effects, mainly temperature and wind velocity, on modal parameter estimates was investigated by many authors, see for instance (Abe *et al.* 2000, Kang *et al.* 2008, Macdonald *et al.* 2005, Li *et al.* 2009). Generally speaking, natural frequencies are usually more affected by temperature variations, while damping ratios might depend upon the mean wind velocity due to the onset of aerodynamic damping (Macdonald *et al.* 2005, Ubertini *et al.* 2010, Ubertini 2010). Several techniques are also available in the literature for modeling the correlation between modal frequencies and ambient temperatures thus allowing the elimination of environmental effects in damage identification based on vibration measurements. Among those methods, the support vector technique (Hua *et al.* 2007) and the neural network technique (Ni *et al.* 2009) are especially worth mentioning, as they proved to be quite effective in practical case studies.

The identification of the modal parameters of the Guangzhou New Television Tower (GNTVT), China, is here performed via a SSI-data approach. To this end, the acceleration measurements made available within the task I of the ANCRiSST benchmark problem (Xia *et al.* 2009, Ni *et al.* 2009) are analyzed, which cover 24 hours of continuous monitoring of the ambient structural response. A particular attention is devoted to the appropriate selection of the main parameters that affect the results of the system identification. Following the findings of previous works (Hong *et al.* 2011), this task is here solved by adopting suitable stability rules and by considering the variability of damping ratios estimates. Once suitable intervals for the variation of the considered parameters are selected, poles pertaining to the same structural modes are grouped by means of an automatic clustering technique, as it is quite usual in the field (e.g., Carden and Brownjohn 2008), and the identified modal parameters are provided with confidence bounds. The overall variability of the results and the effects of ambient conditions (ambient temperature and mean wind velocity) are investigated by analyzing several data sets, obtained by subdividing the available acceleration histories into sub-intervals of appropriate lengths. In particular, both 10 minutes and 1 hour long records are considered. Finally, the capability of the considered identification strategy in correctly identifying all the structural modes comprised within the specified frequency range is checked by comparing modal parameter estimates with preliminary finite element predictions.

The techniques adopted in this paper, i.e., SSI and clustering analysis, are well-known and it is not in the intentions of the authors to deal with substantial modifications of these methods. On the contrary, the study is meant to present their application to an extraordinary case study, which is quite relevant both in terms of structural audacity and in terms of the complexity of the structural health monitoring (SHM) system (Ni *et al.* 2009). The results presented in this paper will thus contribute to the definition of reliable baseline modal parameters of the structure to be employed for future engineering purposes (e.g., finite element model (FEM) updating and damage detection) and shall be helpful to test the performances of the considered techniques for system identification by comparison with the results obtained by different researchers involved in the benchmark problem.

2. Governing relations

The necessary background on Stochastic Subspace Identification is briefly recalled here for the sake of clarity. For more extensive details the reader is referred to the original work by Van Overschee and De Moor (1996) and to the paper by Alicioğlu and Lus (2008).

Let us consider the linear dynamics of a time-invariant N -dof structural system. The equations of motion can be expressed in first order form and discrete time $t = k\Delta t$, Δt being the sampling time and k being the generic time step, as

$$\begin{aligned}\mathbf{x}(k+1) &= \mathbf{A}\mathbf{x}(k) + \mathbf{w}(k) \\ \mathbf{y}(k) &= \mathbf{C}\mathbf{x}(k) + \mathbf{v}(k)\end{aligned}\tag{1}$$

where $\mathbf{x} \in \mathfrak{R}^n$ is the state vector, $\mathbf{y} \in \mathfrak{R}^1$ is the vector of output measurements, $\mathbf{A} \in \mathfrak{R}^{n \times n}$ is the system matrix, containing the information on the second-order mass, damping and stiffness matrices, and $\mathbf{C} \in \mathfrak{R}^{1 \times n}$ is the output matrix. In Eq. (1) it is also assumed that the structure is subjected to a white noise process vector $\mathbf{w} \in \mathfrak{R}^n$ while the measurements are affected by a white noise process

vector $\mathbf{v} \in \mathfrak{R}^l$.

Stochastic system identification algorithms aim at determining the model's order n and the system matrices \mathbf{A} and \mathbf{C} using the measurements $\mathbf{y}(0), \mathbf{y}(1), \dots, \mathbf{y}(s-1)$ available in s time steps. Once these quantities have been estimated, the h -th circular natural frequency ω_h , the h -th modal damping ratio ξ_h and the h -th complex mode shape Φ_h can be determined as

$$\begin{aligned}\omega_h &= \frac{|\ln(\lambda_h)|}{\Delta t} \\ \xi_h &= \frac{-\text{Re}[\ln(\lambda_h)]}{\omega_h \Delta t} \\ \Phi_h &= \mathbf{C}\Psi_h\end{aligned}\quad (2)$$

where λ_h and Ψ_h denote the h -th complex eigenvalue and eigenvector of matrix \mathbf{A} with $\text{Re}[\lambda_h] > 0$.

Data driven stochastic subspace decomposition methods require the construction of the block Hankel matrix \mathbf{H} , having $2i$ block rows and j columns, with $l \cdot i \geq n$ and $j \leq s - 2i + 1$, which is defined as

$$\mathbf{H} = \begin{bmatrix} \mathbf{y}(0) & \mathbf{y}(1) & \cdots & \mathbf{y}(j-1) \\ \mathbf{y}(1) & \mathbf{y}(2) & \cdots & \mathbf{y}(j) \\ \vdots & \vdots & \ddots & \vdots \\ \mathbf{y}(i-1) & \mathbf{y}(i) & \cdots & \mathbf{y}(i+j-2) \\ \mathbf{y}(i) & \mathbf{y}(i+1) & \cdots & \mathbf{y}(i+j-1) \\ \mathbf{y}(i+1) & \mathbf{y}(i+2) & \cdots & \mathbf{y}(i+j) \\ \vdots & \vdots & \cdots & \vdots \\ \mathbf{y}(2i-1) & \mathbf{y}(2i) & \cdots & \mathbf{y}(2i+j-2) \end{bmatrix} = \begin{bmatrix} \mathbf{Y}_p \\ \mathbf{Y}_f \end{bmatrix}\quad (3)$$

It can be observed that the calculation of matrix \mathbf{H} as in Eq. (3) essentially corresponds to an implicit calculation of output covariances (Peeters and De Roeck 2000). Matrices $\mathbf{Y}_p \in \mathfrak{R}^{li \times j}$ and $\mathbf{Y}_f \in \mathfrak{R}^{li \times j}$ in Eq. (3) are referred to as “past” and “future” output block matrices. The orthogonal projection of the row space of \mathbf{Y}_f onto the row space of \mathbf{Y}_p , which is denoted by $\mathbf{P}_i = \mathbf{Y}_f / \mathbf{Y}_p$, can be directly calculated yielding a matrix $\mathbf{P}_i \in \mathfrak{R}^{li \times j}$ which can be also expressed as

$$\mathbf{P}_i = \Gamma_i \hat{\mathbf{X}}_i = \begin{bmatrix} \mathbf{C} \\ \mathbf{CA} \\ \vdots \\ \mathbf{CA}^{i-1} \end{bmatrix} [\hat{\mathbf{x}}_i \quad \hat{\mathbf{x}}_{i+1} \quad \cdots \quad \hat{\mathbf{x}}_{i+j+l}] \quad (4)$$

Γ_i being the observability matrix of the system and $\hat{\mathbf{X}}_i$ being a matrix that contains Kalman filter estimates, denoted by the over-hat $\hat{\bullet}$, of the state vector at different time steps. Eq. (4) constitutes the main theorem of stochastic subspace decomposition. Indeed, by virtue of Eq. (4), both Γ_i and $\hat{\mathbf{X}}_i$ can be calculated by means of the singular value decomposition (SVD) of the formerly calculated matrix \mathbf{P}_i . Then, the system matrices \mathbf{A} and \mathbf{C} are readily extracted from the observability matrix Γ_i .

The available SSI-data algorithms essentially differ for the weighting matrices applied to the projection matrix before the SVD. On this respect, the well-known canonical variate based algorithm (CVA) is

here adopted as it was shown to yield superior performances if compared to different approaches (Alicioğlu and Lus 2008).

3. Adopted system identification technique

Following relevant literature works, the classic CVA algorithm by Van Overschee and De Moor (1996) is adopted in this paper alongside with a noise mode elimination procedure and a clustering analysis. SSI and clustering analysis are indeed quite often used in the literature (e.g., Carden and Brownjohn, 2008) due to their effectiveness in providing reliable modal parameter estimates. Moreover, the approach adopted in this paper is essentially similar to that adopted in (Hong *et al.* 2011) which already proved to be quite effective in the case of a complex structure represented by a long-span suspension bridge.

As explained in Section 2, the CVA algorithm (Van Overschee and De Moor 1996) requires the preliminary tuning of, at least, three fundamental parameters which may strongly affect the outcome of the identification process. These parameters are:

1. the number i of output block rows in Eq. (3)
2. the number j of output block columns of matrix \mathbf{H} in Eq. (3)
3. the order n of the model (i.e. the dimension of the state vector which equals the number of system eigenvalues).

The number j of output block columns has to be as large as possible and, as it has been discussed in Section 2, its maximum value is directly related to the total number of time steps available in the measurements. Here, only the maximum possible value of $j = s-2i+1$ is considered and variations of such a parameter are not accounted for. It is also worth noting that, although model's order is obviously an inherent property of the system, which could be determined on the basis of SVD, it is always unknown when working with ambient data and, so, some criterion to determine feasible values of n must be sought. As it will be better explained in the following developments of this work, stabilization diagrams (SDs) and damping variations are considered here for this purpose, as suggested in other literature works (e.g., Hong *et al.* 2011).

Different values of the aforementioned main parameters are here considered. In particular, i is varied in an interval $[i_{min}, i_{max}]$ with step amplitude Δi and n is varied in an interval $[n_{min}, n_{max}]$ with amplitude Δn . Modal parameters are then extracted for each combination of i and n . By operating in this way, a large number of modal parameter estimates become available. Unfortunately, only some of these poles correspond to structural modes while the remaining ones are related to noise. Therefore, a tool for discriminating structural from noise modes is required to make order. To this end, the method described below is here adopted.

First of all, a mode whose mode shape is not similar to the mode shapes of at least 2 other modes is regarded as a noise mode and eliminated. To this end, the modal assurance criterion (MAC) is applied to all possible pairs of identified modes and two eigenvectors are regarded as similar if their MAC value is greater than $1-\varepsilon_{MAC,noise}$, $\varepsilon_{MAC,noise}$ being a small tolerance here assumed as 0.01. Therefore, a specific mode is eliminated if there are not at least 2 other modes which have a MAC value, with respect to the considered mode, higher than $1-\varepsilon_{MAC,noise}=0.99$. The choice $\varepsilon_{MAC,noise}=0.01$ is made under the assumption that two eigenvectors with a MAC value greater than 0.99 are almost perfectly correlated (perfect correlation corresponds to a MAC value equal to 1). As a second step, the percentage frequency difference is calculated for each possible pair of identified modes. Then,

all modes that have less than 3 other modes with relative frequency differences smaller than a given tolerance $\varepsilon_{f,noise}$ (assumed as 0.02) are regarded as noise modes. Thirdly, the remaining modes are grouped by means of a clustering technique. To this end, modes pertaining to a single group (cluster) are chosen in such a way to have relative frequency differences, relative damping differences and 1-MAC values, calculated with respect to a reference mode of the cluster, that are smaller than given tolerances ε_f (assumed as 0.01), ε_ξ (assumed as 0.03) and ε_{MAC} (assumed as 0.01), respectively. The reference mode is here chosen as the one corresponding to the smallest order and the smallest number of output block rows inside each cluster. Obviously, the same mode cannot belong to more than one cluster. Finally, clusters containing less than 3 modes or having average damping ratios larger than 50% are further eliminated.

4. Field measurements

The GNTVT, recently constructed in Guangzhou, China, is a super-tall structure (Fig. 1(a)) with the height of 610 m (Xia *et al.* 2008, Ni *et al.* 2009). It is a tube-in-tube structure which comprises a reinforced concrete inner tube and a steel outer one constructed by adopting concrete-filled-tube (CFT) columns style (Fig. 1(b)). The outer tube consists of 24 CFT columns, uniformly spaced in an elliptical shape while inclined in the vertical direction. The elliptical outer section decreases with the height from $50\text{ m} \times 80\text{ m}$ at ground level to the minimum dimensions of $20.65\text{ m} \times 27.5\text{ m}$ at 280 m height; then, it increases again to $41\text{ m} \times 55\text{ m}$ at the top level of the tube (454 m height), changing its horizontal orientation with the height (the top ellipse is rotated clockwise by 45° relative to the bottom oval in the horizontal plane) as shown in Fig. 1(c). The columns are interconnected transversely by steel ring beams and bracings. Thirty-six floors and connection girders allow linking

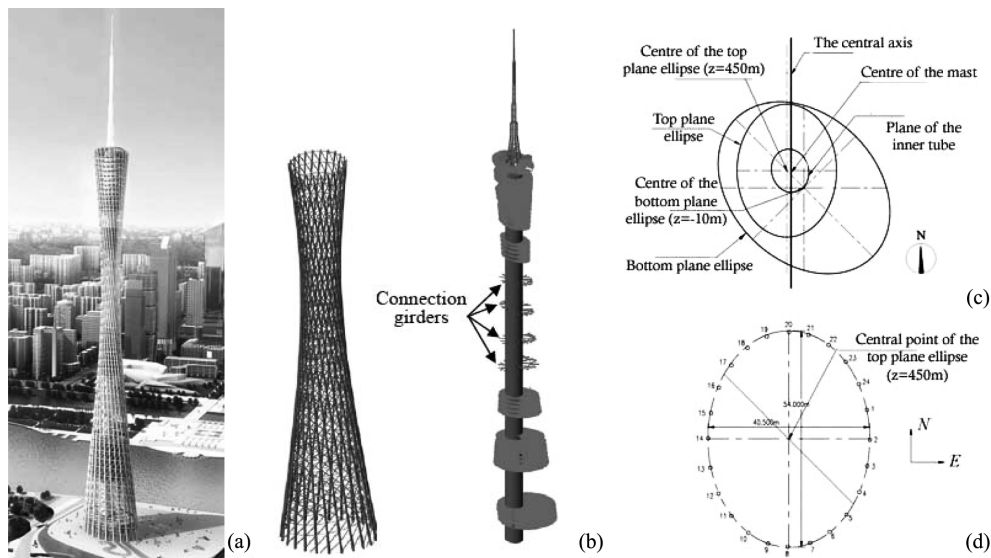


Fig. 1 GNTVT: (a) rendering view of the tower, (b) outer-tube, inner-tube with floors, connection girders and mast, (c) geometrical representation of the outer-tube changing in dimension and orientation, (d) zoomed view of the outer-tube top section at $z = 450\text{ m}$

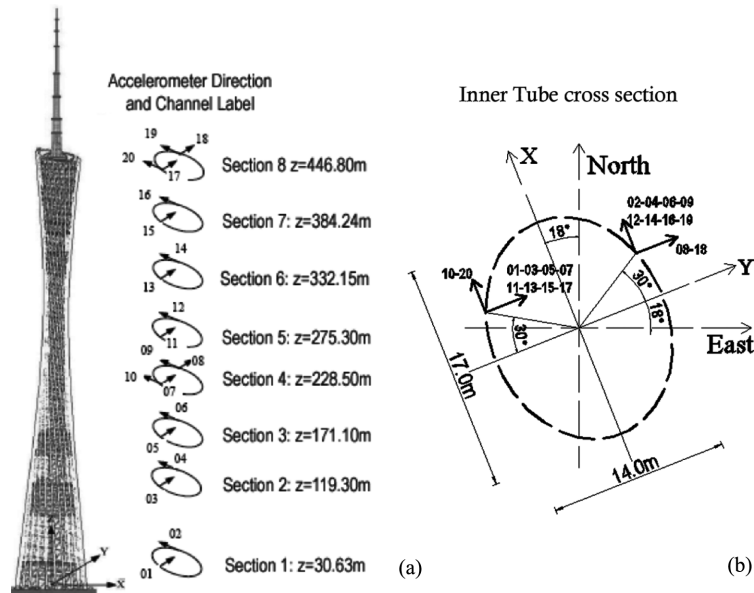


Fig. 2 Accelerometers sensors location on the GNTVT (a) position of the accelerometers on the 8 levels, (b) plan position of the accelerometers with the measurements directions and the channel labels

the outer tube with the inner tube which has an oval shape as well but with constant dimensions of $14\text{ m} \times 17\text{ m}$ (Fig. 1(c), where the inner tube is the smallest oval section).

A structural health monitoring system consisting of 16 types of more than 700 sensors was designed and implemented by the Consortium of Hong Kong Polytechnic University and Sun Yat-Sen University on GNTVT for both in-construction and in-service real-time monitoring. For this purpose a SHM benchmark problem was conceived (Xia *et al.* 2008, Ni *et al.* 2009) by considering the GNTVT as the test structure and using real time measurement data, recorded by a variety of different sensors including accelerometers, strain gauges and GPS systems that are currently receiving much attention (Casciati and Fuggini 2009a, 2009b). A dense range of twenty uni-axial accelerometers were placed at 8 sections at different heights of the tower inner tube as depicted in Fig. 2(c). On each of the eight sections two accelerometers were installed, located at the edges of the inner tube section, forming an angle of 30° with the horizontal short axis direction of the inner tube. The two uni-axial accelerometers allow, for each level, measurements of the vibrations along the long and the short axis of the inner tube, respectively (i.e., X and Y directions, respectively). Only at sections 4 and 8, four uni-axial accelerometers were installed, located in two points of the inner tube section, allowing to record two acceleration measurements for the long-axis of the inner tube and two for the short-axis. It is worth noting that the long-axis and the short-axis of the inner tube are rotated horizontally of an angle of 18° with respect to the North and to the East directions (which also coincide with the long and short axis of the outer tube top section), respectively, as depicted in Fig. 2.

Twenty-four hours of ambient vibration records, subdivided in temporal windows of one hour length (for a total of 24 data sets), were made available within the task I of the benchmark. The measurements were performed from January 19th to January 20th 2010, starting from 5:00 pm. At that time the entire structure was completed. An anemometer and a thermocouple were also

installed at the top of the main tower ($z = 641.1$ m) which recorded the wind speed, the wind direction and the ambient temperature.

5. Modal identification of the GNTVT

The system identification of the GNTVT is carried out by using the field measurements described in Section 4. As a first screening, it was decided to analyze 5 of the available 24-hours data, and divide them into sub-intervals of 10-minutes length that were chosen to be spread along the entire 24 hours records. A total of 30 windows, 600-seconds long, were thus obtained (i.e., 30 data sets). This analysis is characterized by a reasonable computational effort and allows to achieve preliminary information for successive refinements. At a first stage of investigation, the available time histories have been down-sampled from 100 Hz to 6.67 Hz. A typical ambient vibration record of acceleration time-history measured on the structure is depicted in Fig. 3, together with its corresponding velocity and displacement time-histories, computed through an integration process.

After determining the modal parameter estimates using 10 minutes long data, each of the 24 hours has been analyzed separately as a single data set 3600-seconds long. The preliminary analysis revealed that the first twelve structural modes are approximately contained in the frequency interval [0-1.25 Hz]. Considering this as a sufficiently large number of modes, only this interval has been retained in the identification process and the information concerning larger natural frequencies has been filtered out by using a lowpass Butterworth filter with cutoff frequency of 1.5 Hz. In the case of the one-hour long records, data have been down-sampled from 100 Hz to 3 Hz so to have a Nyquist frequency of 1.5 Hz, which is slightly greater than the largest frequency of interest (1.25 Hz), and a frequency resolution of $2.78 \cdot 10^{-4}$ Hz. As better explained in the following developments of this work, this choice also permitted to emphasize the role played by the length of the records on the repeatability of the modal parameter estimates.

In the case of the 10-minutes data, having a total of $l=20$ output measurements of length $s=600 \cdot 6.67$, being 6.67 Hz the sampling frequency, reflects on a maximum number of block rows of the Hankel matrix, i_{max} , which results from the condition $2i \leq (s+1)/(l+1)$, thus being $i \leq 95$. Choosing Δi as about 1/10 of i_{max} , i_{min} is taken as $i_{max} - 4 \cdot \Delta i$, so to have 5 values of i . Here, i_{max} is chosen as 90, Δi as 10 and i_{min} as 50. In order to comprise the computational effort within reasonable limits, the same parameters are also considered in the case of the one-hour long records.

The range of variability of model's order is chosen on the basis of SDs, i.e., plots of the identified frequencies against n , and damping variations. SDs permit to highlight the modes whose properties do not change significantly when varying the dimension of the state vector (stable modes). An example of SD, calculated for a sample 10 minutes record, is shown in Fig. 4 (left). In this plot a

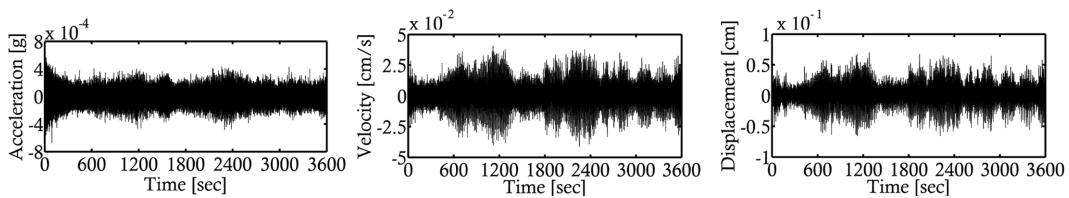


Fig. 3 Sample acceleration record (left) and corresponding velocity (middle) and displacement (right) time-histories

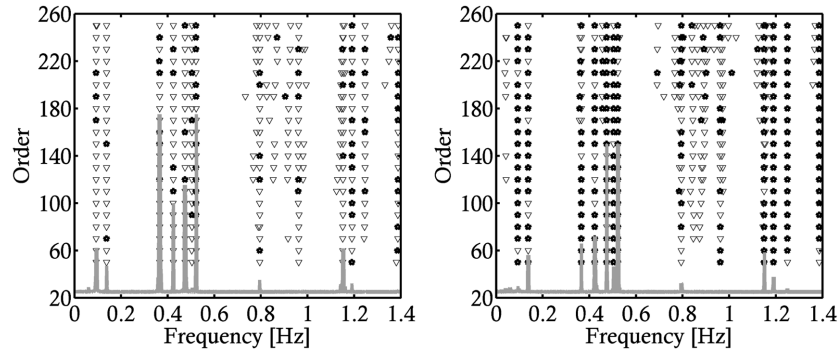


Fig. 4 Sample stabilization diagrams: 10 minutes record (left), 1 hour record (right)

pole that is consistent (i.e., similar) with a two order larger model in terms of frequency, damping ratio and mode shape, is denoted with a black star, while a pole that only satisfies frequency and mode shape similarity checks is denoted with a gray triangle. In the similarity checks the tolerances $\varepsilon_f = 0.01$ (for relative frequency differences), $\varepsilon_\xi = 0.03$ (for relative damping differences) and $\varepsilon_{MAC} = 0.01$ (for 1-MAC values) are adopted. The right plot in Fig. 4 is, on the contrary, calculated by considering a sample 1 hour long record. For a better visualization of the different modes, also the power spectral density (PSD) functions of the 20 measurements are plotted in the figure (grey lines).

The presented results show that structural modes which are consistent in terms of damping ratios are more easily identified using longer data records rather than using shorter ones. This circumstance was also confirmed by different authors (e.g., by Carden and Mita 2009). Moreover, most of the modes fail to appear consistently for $n < 50$. No clear indication is obtained from these plots on some maximum value of the model's order. Therefore, these results indicate that n_{min} should be chosen to be larger than 50 and n_{max} might be freely chosen. It is important to note, however, that this last conclusion is not general but it is strictly related to the considered case study.

In order to make a more appropriate decision on the adopted range of n , the variation of damping ratios with such a parameter is also worth investigating (Hong *et al.* 2011). Fig. 5 shows similar plots for the first two structural modes and for a sample one-hour long data set. These plots indicate that damping ratios estimates appear to be sufficiently stable along model's order in the order range [100, 200]. Under the assumption that in the optimal range of variability of n the “true” damping ratios should appear consistently with small variations, it is decided to limit the maximum value of

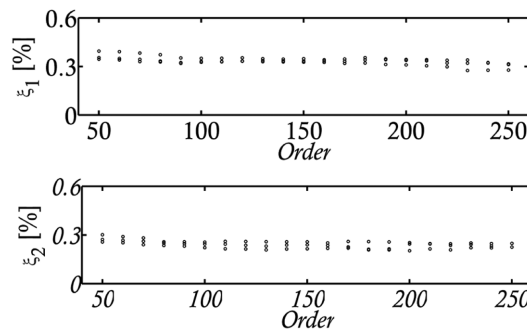


Fig. 5 Estimated damping ratios of the first two modes as functions of model's order

n to 200 and the interval [$n_{min}=140$, $n_{max}=200$] is finally chosen with step amplitude $\Delta n=10$.

As already mentioned, in the frequency range below 1.25 Hz a total of 12 structural modes are identified. As an example, in the left plot of Fig. 6 identified damping ratios are plotted vs. identified frequencies for a sample data set using one-hour long records. In this plot the crosses indicate the mean values of each cluster, while the lines parallel to the vertical axis indicate the amplitudes of the 95% confidence intervals of the damping ratios calculated for the different values of n and i . The amplitudes of these confidence intervals are so small that they can be appreciated only in detailed views, such as in two cases shown in Fig. 6. The 95% confidence intervals of the natural frequencies are also reported in Fig. 6, as lines parallel to the horizontal axis, but they are not visible even in the detailed views. These circumstances show that, for a single data set, the variations of damping ratios estimates and natural frequencies with n and i are, in the considered case, very small. The identified modal parameters (mean values) among all the considered one-hour long data sets are shown in the right plot of Fig. 6. The identified mode shapes are presented in the successive developments of this work.

It is important to mention that the confidence bounds shown in Fig. 6 reflect the uncertainties associated with different choices of n and i , but do not necessarily reflect the statistical accuracy of the modal parameter estimates with regard to the available data, as considered by other authors (Reynders *et al.* 2008, Carden and Mita 2009), which would go beyond the purposes of the present investigation. In order to quantify, to some extent, the uncertainties associated with the modal parameter estimates, the variations of the results obtained in different data sets are here investigated. To this end, the mean values and the coefficients of variation (CVs) of the identified modal frequencies f_i ($i=1,2,\dots,12$) and damping ratios ξ_i ($i=1,2,\dots,12$) among the considered data sets are provided in Table 1 and 2. The results show that the variability of identified frequencies is very low (CVs of about 0.15% as an average and 0.36% as a maximum, in the case of one-hour records).

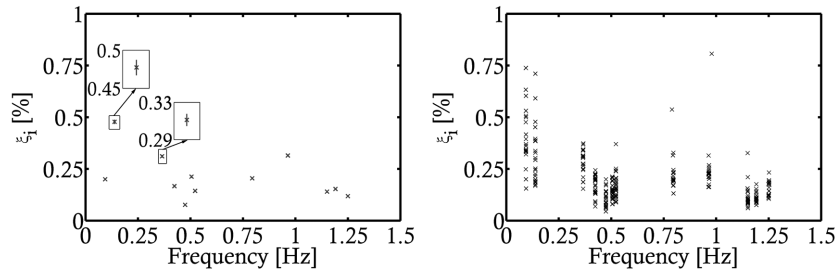


Fig. 6 Identified modal parameters for a sample data set (left), identified modal parameters for all the considered data sets (right)

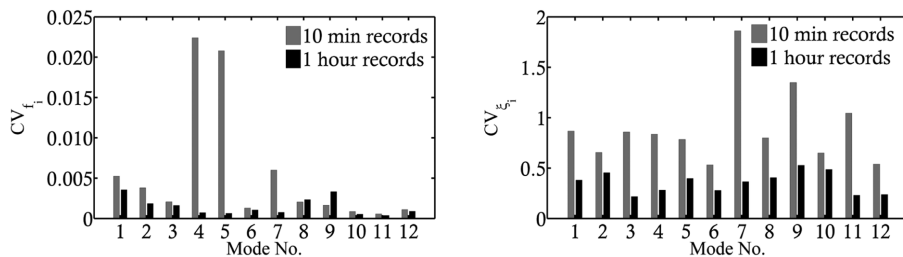


Fig. 7 Coefficients of variation of natural frequencies (left) and damping ratios (right) for different lengths of data sets

Table 1 Mean values and coefficients of variation of identified modal frequencies among the different data sets (values in Hz)

No.	f_1	f_2	f_3	f_4	f_5	f_6	f_7	f_8	f_9	f_{10}	f_{11}	f_{12}
10-minutes records, 30 data sets												
Mean	0.0935	0.1383	0.3659	0.4257	0.4727	0.5052	0.5217	0.7950	0.9648	1.1505	1.1908	1.2496
CV	0.0053	0.0038	0.0021	0.0224	0.0208	0.0013	0.0060	0.0020	0.0016	0.0009	0.0006	0.0011
1-hour records, 24 data sets												
Mean	0.0936	0.1384	0.3659	0.4238	0.4747	0.5054	0.5224	0.7951	0.9656	1.1505	1.1910	1.2506
CV	0.0036	0.0019	0.0016	0.0007	0.0006	0.0011	0.0008	0.0023	0.0033	0.0005	0.0004	0.0009

Table 2 Mean values and coefficients of variation of identified modal damping ratios among the different data sets (values in percentage)

10-minutes records, 30 data sets												
No.	ξ_1	ξ_2	ξ_3	ξ_4	ξ_5	ξ_6	ξ_7	ξ_8	ξ_9	ξ_{10}	ξ_{11}	ξ_{12}
Mean	0.6965	0.5349	0.2502	0.2300	0.1779	0.1929	0.3077	0.2846	0.3076	0.1379	0.1668	0.2275
CV	0.8672	0.6552	0.8574	0.8360	0.7838	0.5321	1.8611	0.7983	1.3484	0.6492	1.0442	0.5393
1-hour records, 24 data sets												
No.	ξ_1	ξ_2	ξ_3	ξ_4	ξ_5	ξ_6	ξ_7	ξ_8	ξ_9	ξ_{10}	ξ_{11}	ξ_{12}
Mean	0.4271	0.3156	0.2631	0.1709	0.1076	0.1441	0.1700	0.2305	0.2552	0.1199	0.1065	0.1531
CV	0.3802	0.4537	0.2290	0.2817	0.3960	0.2791	0.3661	0.4050	0.5273	0.4863	0.2303	0.2372

This means, for instance, that using the adopted SSI method a damage detection technique based on frequency variations would be able to detect minimal levels of damages which produce frequency changes of the order of 0.15%. On the contrary, the variability of damping ratios is much higher than that of natural frequencies, with average CVs, among the different data sets, of about 35% in the case of one-hour records. A similar result was somehow expected because, as it is well-known, estimates of damping ratios are usually more scattered than estimates of natural frequencies (Alicioglu and Lus 2008). Moreover, the CVs of damping ratios estimates are very close to those obtained in similar studies in the literature (see for instance (Nayeri *et al.* 2008, Li *et al.* 2009)). On this respect, it is very important to note that damping variability is much smaller in the case of one-hour long records than in the case of ten-minutes records, where the average CV is about 60%. Similarly, the variability of natural frequencies is also improved in the former case. For instance, Fig. 7 shows a comparison between the coefficients of variation of natural frequencies CV_{f_i} and damping ratios CV_{ξ_i} for the different structural modes in both cases of ten-minutes long records and one-hour records. Looking at these results, it is concluded that modal parameter estimates, and particularly modal damping ratios, using ten-minutes long records exhibit a level of uncertainty which is not acceptable and, so, only the results obtained using one-hour long records are considered in the successive developments of this paper.

As already mentioned, the identified mode shapes are presented later on in this study. At this stage, however, it is important to mention that the mode shapes identified in the different data sets also exhibited some small variations which are a little more significant in the case of lower modes than in the case of higher order ones. As an example, Fig. 8 presents the average MAC values of the identified mode shapes with respect to those identified within a reference data set (the data set recorded at noon on January 20th 2010) in the case of the one-hour long records. In such a Figure,

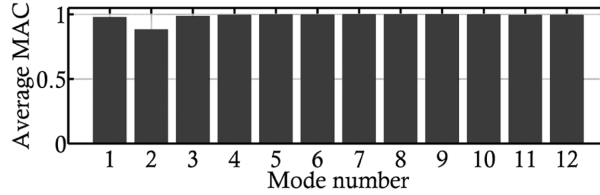


Fig. 8 Average MAC values of identified mode shapes with respect to the mode shapes identified in a reference data set

the average MAC values are always greater than 97.7%, showing modest variations of the mode shapes among the different data sets, with the only exception of mode 2 for which the average MAC is equal to 88.4%. This last value entails that the variation of this mode shape among the different data sets is not insignificant. Possible reasons for this outcome are a small excitation level of this mode, the finite length of the data records, or an insufficient number of sensors. However, considering that most of the MAC values in Fig. 8 are very close to 1, it is concluded at this stage that the observed variations of the identified mode shapes are fully acceptable. It is also important to mention that a check performed aside has shown that the results presented in Fig. 8 would not be substantially modified by changing the reference data set.

6. Environmental effects on modal parameter estimates

A key point in view of future damage detection and health assessment applications is to investigate the influence of environmental factors on the estimated modal parameters. To this end, the effect of ambient temperature on the estimated modal frequencies and the effect of the mean wind velocity on the estimated damping ratios are here analyzed.

Figs. 9 and 10 show the percentage variations f_i of the i -th modal frequencies f_i with ambient temperature T . In such plots, linear interpolating lines are also shown. Although slight temperature variations were observed during the tests, the resulting frequency variations are not insignificant (of the order, in some cases, of 0.5%) and some trends can be clearly recognized in the lower modes, which generally confirm that, as usual, natural frequencies decrease with increasing temperature (Abe *et al.* 2000, Kang *et al.* 2008). A larger scatter of lower frequencies with respect to higher order ones is also evidenced in these plots.

The percentage variations $\Delta\xi_i$ of the i -th modal damping ratios ξ_i ($i=1,2,\dots,12$) with the X and Y components of the mean wind velocity are shown in the plots of Figs. 11 and 12. In these cases, the data scatter is much larger than that observed in natural frequencies which does not allow yielding general conclusions. However, some modes exhibit increasing or decreasing trends of damping ratios with the X and/or Y components of the mean wind velocity. Obviously it is not easy, at this stage, to conclude whether these trends are effectively due to the onset of aerodynamic damping, which usually plays a significant role in flexible structures (Cluni *et al.* 2007, Ubertini 2010) and varies with the mean wind velocity (being it positive or negative), or if they are simply caused by meaningless experimental scatter. Probably, in the presented case, both aspects are influencing the results.

Although a definitive conclusion about wind velocity effects cannot be derived from the results presented in Figs. 11 and 12, it is worth noting that some modal damping ratios are almost stable

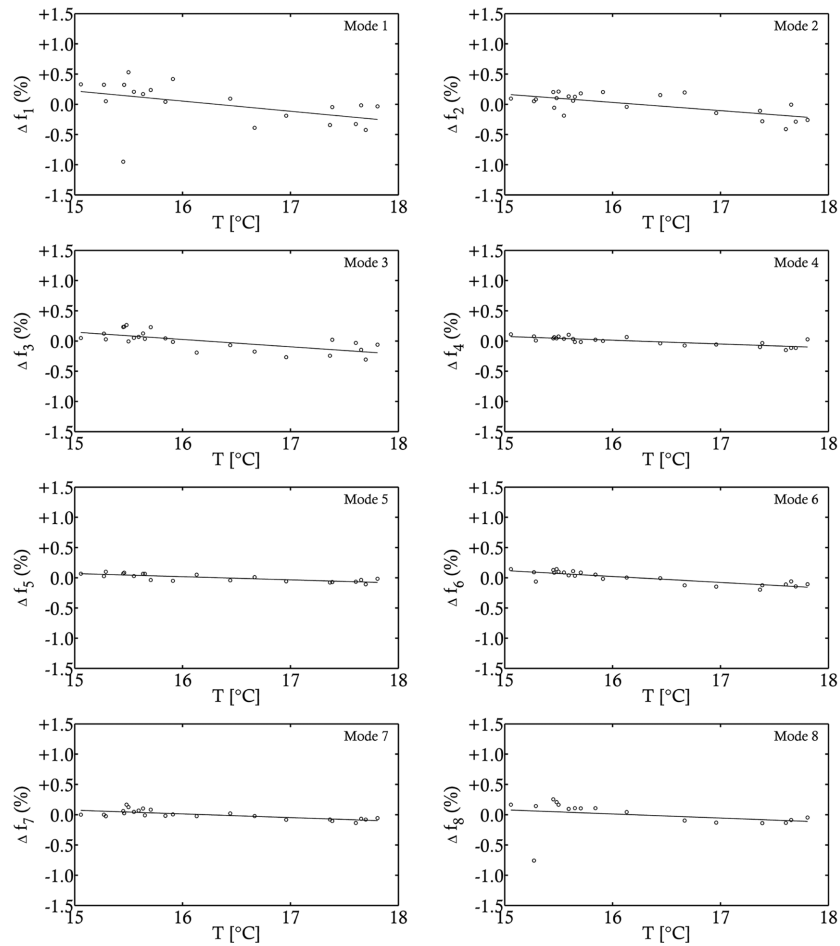


Fig. 9 Variation of natural frequencies with ambient temperature (modes 1-8)

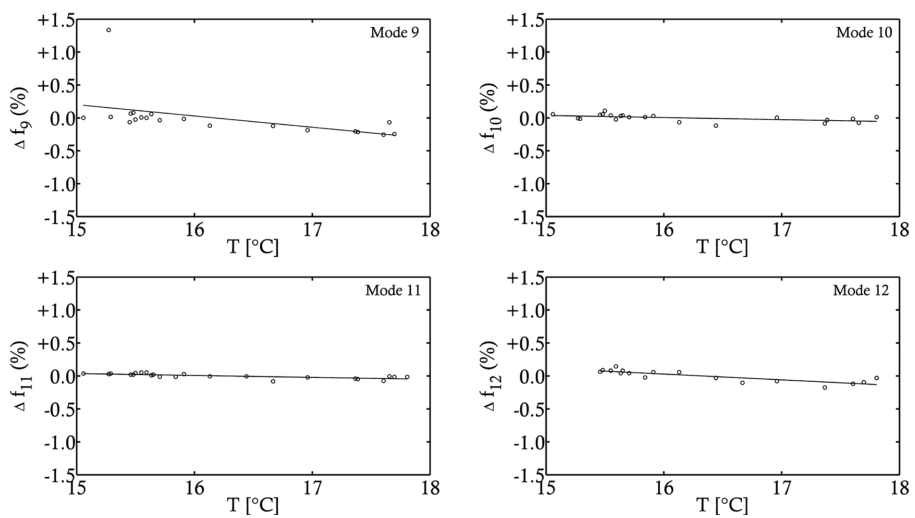


Fig. 10 Variation of natural frequencies with ambient temperature (modes 9-12)

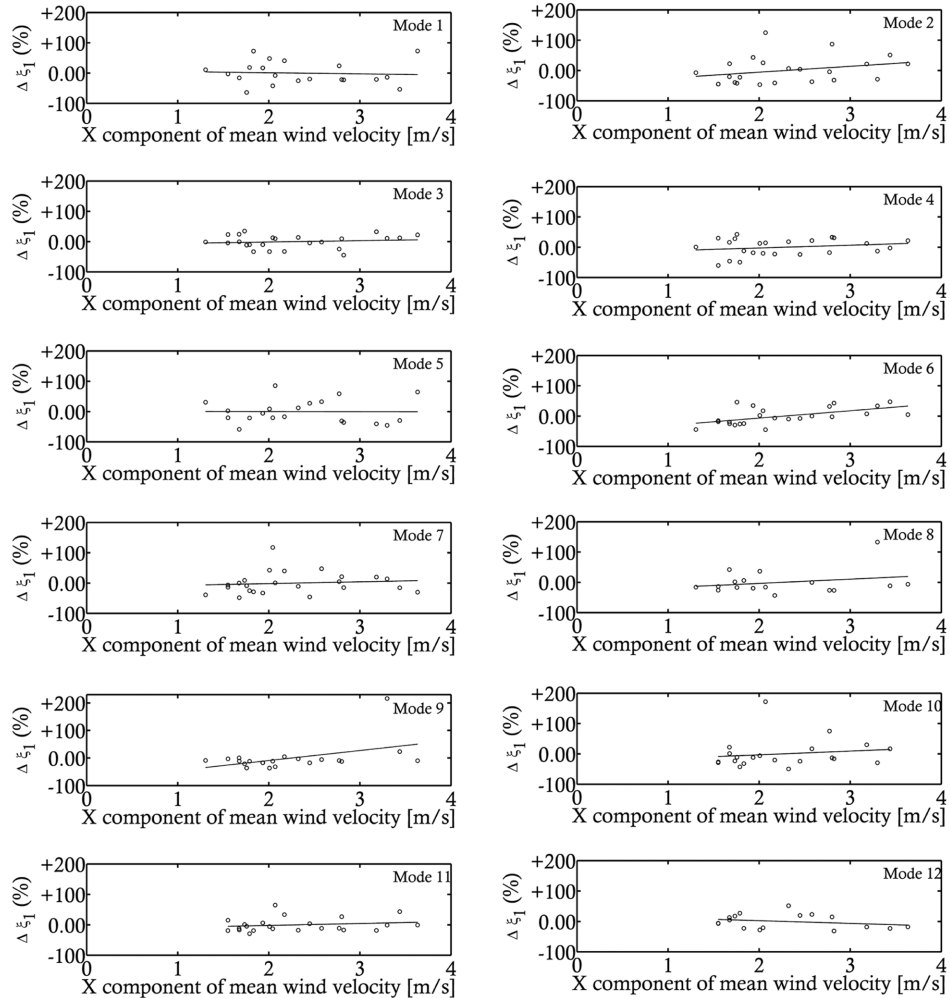


Fig. 11 Variation of damping ratios with X component of mean wind velocity

with both components of the mean wind velocity. This result seems to confirm the expected circumstance that the aerodynamic damping is likely negligible in the present case, considering that the observed values of the mean wind velocity are very small. In the meanwhile, the damping ratios of some modes exhibit clear trends with one component of the mean wind direction while being almost constant with the orthogonal wind component (see for instance mode 2). This seems to be a stronger indication of the aeroelastic nature of these trends: for instance, in the case of mode 2, as it will be clearer in the following developments of the work, the leading vibration component is in the X direction which would be consistent with the trend observed in Fig. 11. However, modes could be found in Figs. 11 and 12 which do not confirm this result.

Looking at the presented results, damping ratios seem to provide average trends with mean wind velocity which are somewhat consistent with what expected in theory. Nevertheless, a much larger number of data sets would be necessary to confirm such conclusion under the assumption that increasing the number of data sets allows compensating the random errors in damping estimations.

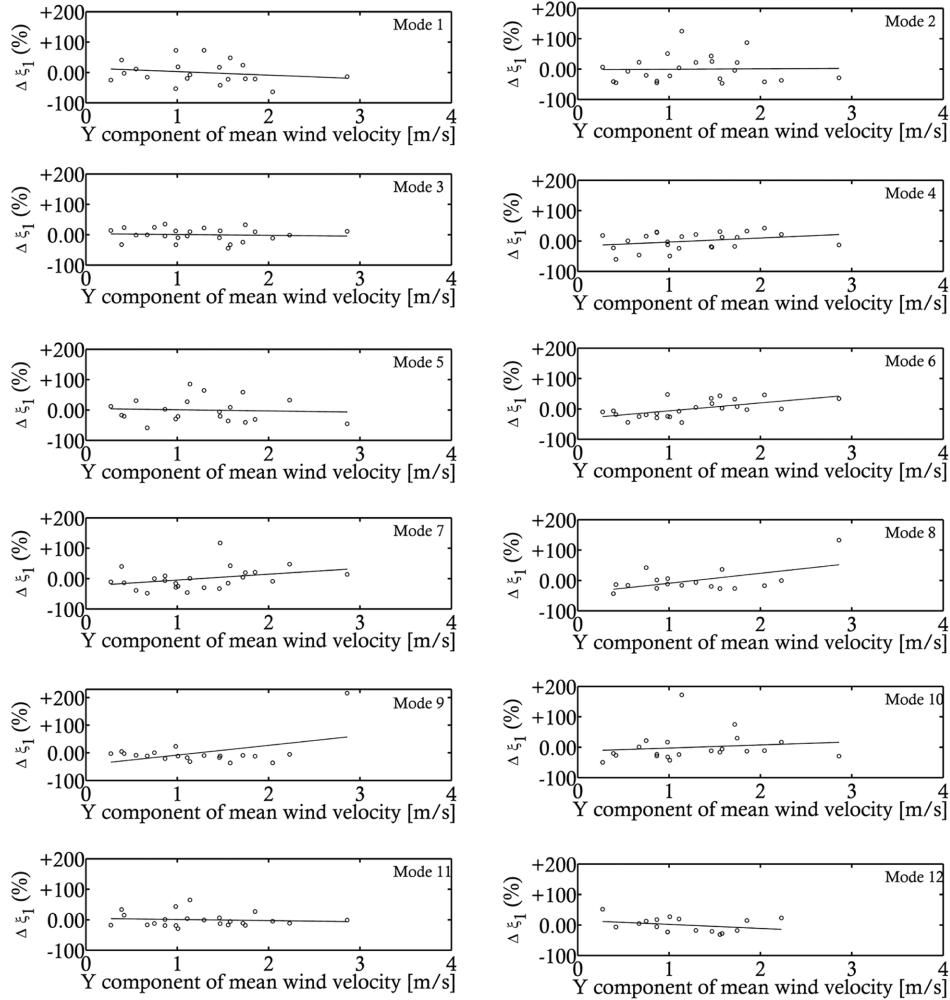


Fig. 12 Variation of damping ratios with Y component of mean wind velocity

7. Comparison with preliminary FEM results

Preliminary finite element (FE) structural matrices of the GNTVT have also been made available within the benchmark problem (Xia *et al.* 2008, Ni *et al.* 2009). It is therefore of interest to compare the FE predictions with the modal parameter estimates obtained from ambient vibration measurements. Since the FE model has not been updated using field measurements it is implicit that identified and calculated modal parameter estimates will unavoidably exhibit some differences. However, the comparison between the two is essential for checking that all the structural modes comprised within the considered frequency interval are effectively identified via SSI-data, in the correct order, and that the identified modal parameters are similar to those expected in the design stage.

Table 3 presents the types of the identified mode shapes (BX denotes a bending mode with a prevailing X component, BY denotes a bending mode with a prevailing Y component, and T denotes

Table 3 Comparison between FE calculated and identified modal parameters; mode type: B (bending), T (torsional)

No.	f_1	f_2	f_3	f_4	f_5	f_6	f_7	f_8	f_9	f_{10}	f_{11}	f_{12}
Mode type	BY	BX	BX	BY	BY	T	BX	BX	BY	BX	BX	T
ID	0.0936	0.1384	0.3659	0.4238	0.4747	0.5054	0.5224	0.7951	0.9656	1.1505	1.1910	1.2506
FE	0.1104	0.1587	0.3463	0.3688	0.3994	0.4605	0.4850	0.7381	0.9026	0.9972	1.0373	1.1218
Δ (%)	17.95	14.67	5.36	12.98	15.86	8.88	7.16	7.17	6.52	13.32	12.91	10.30
MAC	0.9793	0.9769	0.7248	0.8927	0.8143	0.9334	0.8716	0.6923	0.7214	0.1010	0.5806	0.6547

a torsional mode) and the comparison between identified (ID) and calculated modal frequencies. Particularly, the identified values correspond to the mean values presented in Table 1 (one-hour long records). Percentage differences between identified and calculated natural frequencies, in Table 3, are denoted by Δ . Overall, these differences are significant (the average percentage frequency difference is about equal to 11%), which is a consequence of the circumstance that the FE model has not been updated. However, considering that there is no clear trend in the values of Δ when varying the order of the modes, that is, the values referred to different modes are almost of the same order of magnitude, it seems that no structural mode is lost in the identification process in the considered frequency range. This conclusion seems to be also corroborated, in most of the cases, by analyzing the MAC values between calculated and identified mode shapes which are also summarized in Table 3. Although it is obvious that the degree of correlation between mode shapes is, in some cases, unavoidably low, which is again a consequence of the circumstance that the FE model has not been updated, it is important to note that MAC values are larger than 90% in the case of modes 1, 2 and 6, are between 80% and 90% in the case of modes 3, 4, 5 and 7 and always larger than 58% with one only exception represented by the 10th mode. It must be mentioned that these results have been obtained by separately scaling the X and Y components of the mode shapes. Particularly, the two components obtained from the FE analysis have been rescaled, here, with respect to their absolute maxima obtained from system identification results. This procedure, although not rigorous because it considers different scaling factors for different components of the same structural modes, allows a better comparison between identified and calculated mode shapes, even without a model updating which is not the subject of this work. In particular, by operating in this way, the calculated MAC values indicate an average between the degree of modal correlation in the X direction and the degree of modal correlation in the Y direction, taken as separate but keeping the information on the phase shift between the X and Y modal components. On the contrary, differences in the levels of modal coupling between these two components are not taken into account, as they are likely to be strongly influenced by modeling uncertainties with the consequence that, dealing with a FE model that has not been updated, might result in a more confused scenario with lower MAC values even when calculated and identified mode shapes correspond to the same structural mode.

The comparison between identified and calculated mode shapes is also shown in Fig. 13. These results clearly show that identified and calculated modes resemble the classic bending eigenfunctions of a cantilever beam, where the peculiar shape of the tower obviously determines a coupling between the vibrations in the X and Y directions. Moreover, the similarity between identified and calculated mode shapes clearly points out for most of the modes from Fig. 13. As shown in Fig. 14, the first two torsional modes of the structure correspond to the 6th and 12th modes.

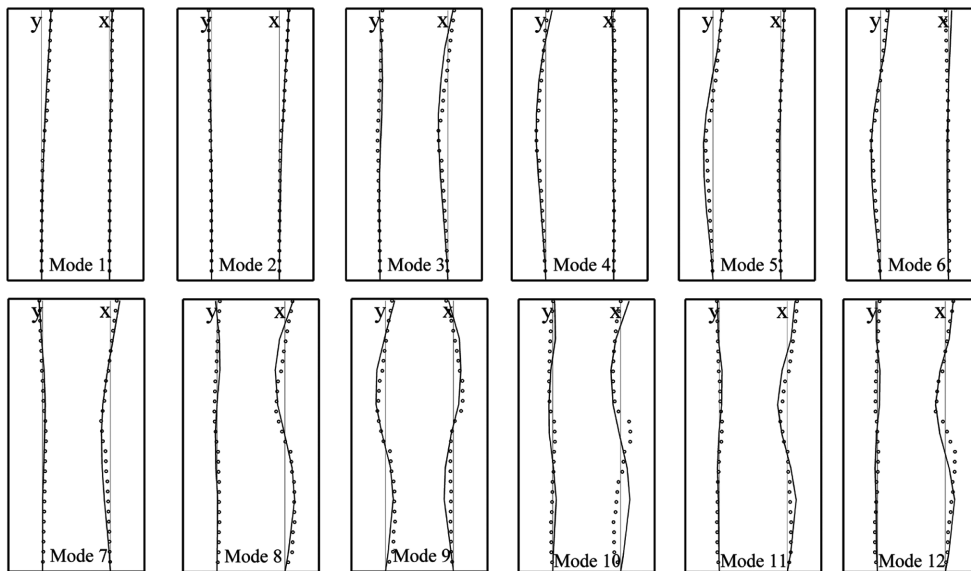


Fig. 13 Identified (continuous lines) vs. FE calculated (black circles) mode shapes

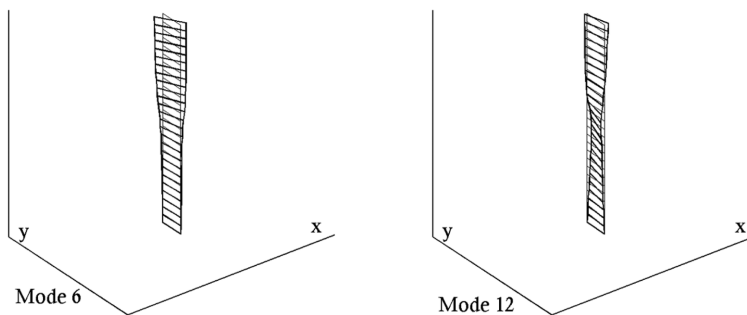


Fig. 14 First two torsional modes (from FE analysis)

8. Conclusions

The identification of the modal parameters of a super high-rise building has been presented via a data driven stochastic subspace approach combined with a noise mode elimination procedure and a mode clustering technique. The results show that by repeating the system identification using records with similar ambient conditions, the obtained frequency estimates have coefficients of variation of about 0.15%, while damping ratios estimates have coefficients of variation of about 35%. In this last case, considering sufficiently long data records was found to be crucial in order to reduce the variability of damping ratios estimates.

The analysis of the role played by ambient conditions has shown that frequency variations due to temperature changes of about 3°C can be clearly appreciated by the considered identification strategy which constitutes an important result in view of future applications of the method. The presented results have also evidenced some trends of some modal damping ratios with mean wind velocity. However, considering the larger scatter affecting estimated modal damping ratios, it is

difficult to discern at this stage whether these trends are effectively caused by aeroelastic effects (i.e., aerodynamic damping) or not. In any case, it is worthwhile to note that, for most of the modes, damping ratios estimates are practically constant, in an average sense, with mean wind velocity. This result confirms the initial guess that aerodynamic damping was likely negligible in the presented case, considering that the measured wind velocities were always very small and comprised between 0 and 4 m/s, and gives some preliminary indication that the errors on modal damping estimates compensate as the number of data sets is increased.

The comparison between preliminary FE predictions and identification results, considering both natural frequencies and mode shapes correlations, seems to confirm that the considered identification strategy allows detecting all the twelve structural modes contained within the considered frequency interval in the correct order.

In summary, the results presented in this paper constitute the essential groundwork for future damage detection applications: the coefficients of variation of natural frequencies and the influence of ambient temperature dictate the minimum level of damage that can be detected using frequency variations; the coefficients of variation of damping ratios estimates are directly related, for instance, to the possibility of separating structural from aerodynamic damping via extrapolation of the observational data for a nil mean wind velocity which, however, would require the availability of field measurements at larger wind velocities.

Acknowledgements

The authors wish to gratefully acknowledge Professor Y.Q. Ni, Hong Kong Polytechnic University, Hong Kong, China, for kindly sharing the information concerning the ANCRiSST monitoring benchmark. Comments and suggestions by Professor R. Betti and Dr. A.L. Hong, Columbia University, New York, and by Professor C. Gentile, Politecnico di Milano, Milano, Italy, are also acknowledged with gratitude.

References

- Abe, M. Fujino, Y., Yanagihara, M. and Sato, M. (2000), "Monitoring of Hakucho suspension bridge by ambient vibration measurement", *Proceedings of SPIE*, **399**, 237-244.
- Alicioğlu, B. and Lus, H. (2008), "Ambient vibration analysis with subspace methods and automated mode selection: case studies", *J. Struc. Engin-ASCE*, **134**(6), 1016-1029.
- Carden, E.P. Brownjohn, J.M.W. (2008), "Fuzzy clustering of stability diagrams for vibration-based structural health monitoring", *Comput-Aided Civ. Inf.*, **23**(5), 360-372.
- Carden, E.P. and Mita, A. (2009), "Challenges in developing confidence intervals on modal parameters estimated for large civil infrastructure with stochastic subspace identification", *Struct. Health Monit.*, DOI:10.1002/stc.358.
- Casciati, F. and Ubertini, F. (2008), "Nonlinear vibration of shallow cables with semi-active tuned mass damper", *Nonlinear Dynam.*, **53**(1-2), 89-106.
- Casciati, F. and Fuggini, C. (2009a), "Towards global positioning system-based structural health monitoring", *Trend. Civil Struct. Eng. Comp.*, (Eds. Topping, B.H.V., Costa Neves, L.F. and Barros, R.C), **15**, 319-352.
- Casciati, F. and Fuggini, C. (2009b), "Engineering vibration monitoring by GPS: long duration records", *Earthq. Eng. Eng. Vib.*, **8**(3), 459-467.
- Chatzi, E.N. and Smyth, A.W. (2009), "The unscented Kalman filter and particle filter methods for nonlinear

- structural system identification with non-collocated heterogeneous sensing”, *Struct. Health Monit.*, **16**(1), 99-123.
- Cluni, F., Gusella, V. and Ubertini, F. (2007), “A parametric investigation of wind-induced cable fatigue”, *Eng. Struct.*, **29**(11), 3094-3105.
- Conte, J.P., He, X., Moaveni, B., Masri, S.F., Caffrey, J.P., Wahbeh, M., Tasbihgoo, F., Whang, D.H. and Elgamal, A. (2008), “Dynamic testing of alfred zampa memorial bridge”, *J. Struct. Eng- ASCE*, **134**(6), 1006-1015.
- Faravelli, L. and Ubertini, F. (2009), “Nonlinear state observation for cable dynamics”, *J. Vib. Control*, **15**(7), 1049-1077.
- Faravelli, L., Fuggini, C. and Ubertini, F. (2009a), “Towards a hybrid control solution for cable dynamics: theoretical prediction and experimental validation”, *Struct. Health Monit.*, **17**(4), 386-403.
- Faravelli, L., Fuggini, C. and Ubertini, F. (2009b), “Experimental study on hybrid control of multimodal cable vibrations”, *Meccanica*, DOI 10.1007/s11012-010-9364-2.
- Faravelli, L., Ubertini, F. and Fuggini, C. (2010), “System identification toward FEM updating of a super highrise building”, *Proceedings of the fifth European Workshop on Structural Health Monitoring*, Sorrento, Italy, June – July.
- Frizzarin, M., Feng, M.Q., Franchetti, P., Soyoz, S., and Modena, C. (2008), “Damage detection based on damping analysis of ambient vibration data”, *Struct. Health Monit.*, **17**(4), 368-385.
- Fuggini, C. (2009), “Using satellites systems for structural monitoring: accuracy, uncertainty and reliability”, Ph.D. Dissertation, University of Pavia, Pavia, Italy.
- Gentile, C. and Gallino, N. (2008). “Ambient vibration testing and structural evaluation of an historic suspension footbridge”, *Adv. Eng. Softw.*, **39**(4), 356-366.
- Hong, A.H., Betti, R. and Lin, C.C. (2009), “Identification of dynamic models of a building structure using multiple earthquake records”, *Struct. Health Monit.*, **16**(2), 178-199.
- Hong, A.L., Ubertini, F. and Betti, R. (2011), “Wind analysis of a suspension bridge: identification and FEM simulation”, *J. Struct. Eng-ASCE*, **137**(1), 133-142.
- Hua, X.G., Ni, Y.Q., Ko, J.M. and Wong, K.Y. (2007), “Modeling of temperature-frequency correlation using combined principal component analysis and support vector regression technique”, *J. Comput. Civil Eng.*, **21**(2), 122-135.
- Kang, S.G., Kwon, J.B., Lee, I.K. and Lee, G.H. (2008). “Structural behaviors of Seohae cable-stayed bridge affected by temperature”, *Proceedings of the 4th International Conference on Bridge Maintenance, Safety and Management*, Seoul, Korea.
- Ko, J.M. and Ni, Y.Q. (2005). “Technology developments in structural health monitoring of large-scale bridges”, *Eng. Struct.*, **27**(12), 1715-1725.
- Li, H., Li, S., Ou, J. and Li, H. (2009), “Modal identification of bridges under varying environmental conditions: temperature and wind effects”, *Struct. Health Monit.*, DOI: 10.1002/stc.319.
- Macdonald, J.H.G. and Daniell, W.E. (2005). “Variation of modal parameters of a cable-stayed bridge identified from ambient vibration measurements and FE modelling”, *Eng. Struct.*, **27**(13), 1916-1930.
- Nayeri, R.D., Masri, S.M., Ghanem, R.G. and Nigbor, R.L. (2008), “A novel approach for the structural identification and monitoring of a full-scale 17-story building based on ambient vibration measurements”, *Smart Mater. Struct.*, **17**(2), 1-19.
- Ni, Y.Q., Xia, Y., Liao, W.J. and Ko, J.M. (2009), “Technology innovation in developing the structural health monitoring system for Guangzhou new TV tower”, *Struct. Health Monit.*, **16**(1), 73-98.
- Ni, Y.Q., Zhou, H.F., and Ko, J.M. (2009), “Generalization capability of neural network models for temperature-frequency correlation using monitoring data”, *J. Struct. Engin-ASCE*, **135**(10), 1290-1300.
- Peeters, B. and De Roeck, G. (2000), “Reference based stochastic subspace identification in civil engineering”, *Inverse Probl.*, **8**, 47-74.
- Peeters, B. and Ventura, C.E. (2003). “Comparative study on modal analysis techniques for bridge dynamic characteristics”, *Mech. Syst. Signal Pr.*, **17**(5), 965-988.
- Pridham, B.A. and Wilson, J.C. (2005), “A reassessment of dynamic characteristics of the Quincy Bay Bridge using output-only identification techniques”, *Earthq. Eng. Struct. D.*, **34**, 787-805.
- Ren, W.X., Peng, X.L. and Lin, Y.Q. (2005), “Experimental and analytical studies on dynamic characteristics

- of a large span cable-stayed bridge”, *Eng. Struct.*, **27**(4), 535-548.
- Reynders, E., Pintelon, R. and De Roeck, G. (2008), “Uncertainty bounds on modal parameters obtained from Stochastic Subspace Identification”, *Mech. Syst. Signal Pr.*, **22**(4), 948-969.
- Ubertini, F. (2008a), “Active feedback control for cable vibrations”, *Smart Struct. Syst.* **4**(4), 407-428.
- Ubertini, F., Hong, A.H., Betti, R. and Materazzi, A.L. (2010), “Identification of wind-excited suspension bridges for SHM: a feasibility study”, *Proceedings of the 34th IABSE symposium*, Venice, Italy, September.
- Ubertini, F. (2010), “Prevention of suspension bridge flutter using multiple tuned mass dampers”, *Wind Struct.*, **13**(3), 235-256.
- Xia, Y., Ni, Y.Q., Ko, J.M. and Chen, H.B. (2008), “ANCRiSST benchmark problem on structural health Monitoring of high-rise slender structures”, *Proceedings of the 4th International Workshop on Advanced Smart Materials and Smart Structures Technologies*, Tokyo, June.
- Van Overschee, P. and De Moor, B. (1996), “Subspace identification for linear systems: Theory-implementation applications”, *Kluwer Academic Publishers*, Dordrecht, The Netherlands.
- Weng, J.H., Loh, C.H. and Yang, J.N. (2009), “Experimental study of damage detection by data-driven subspace identification and finite-element mode updating”, *J. Struc. Engin-ASCE*, **135**(12), 1533-1544.
- Wong, K.Y. (2004), “Instrumentation and health monitoring of cable-supported bridges”, *Struct. Health Monit.*, **11**(2), 91-124.